Gateway Placement and Packet Routing For Multihop In-Vehicle Internet Access

Hassan Aboubakr Omar, *Student Member, IEEE,* Weihua Zhuang, *Fellow, IEEE,* and Li Li, *Senior Member, IEEE*

Abstract—In-vehicle Internet access is one of the main applications of vehicular ad hoc networks (VANETs), which aims at providing the vehicle passengers with a low-cost access to the Internet via on-road gateways. This paper introduces a new strategy for deploying Internet gateways on the roads, together with a novel scheme for data packet routing, in order to allow a vehicle to access the Internet via multihop communications in a VANET. The gateway placement strategy is to minimize the total cost of gateway deployment, while ensuring that a vehicle can connect to an Internet gateway (using multihop communications) with a probability greater than a specified threshold. This cost minimization problem is formulated by using binary integer programming, and applied to a realistic city scenario, consisting of the roads around the University of Waterloo. To the best of our knowledge, the proposed deployment strategy is the first study to address the probability of multihop connectivity among the vehicles and the deployed gateways. On the other hand, the developed packet routing scheme is based on a multichannel medium access control protocol, known as VeMAC [1], [2], using time division multiple access. The performance of this cross-layer design is evaluated for a multichannel VANET in a highway scenario, mainly in terms of the end-to-end packet delivery delay. The end-to-end delay is calculated by modeling each relay vehicle as a queueing system, in which the packets are served in batches of no more than a specified maximum batch-size. The proposed gateway placement and packet routing schemes represent a step toward providing reliable and ubiquitous in-vehicle Internet connectivity.

Index Terms—Gateway placement, packet routing, TDMA, delay analysis, and vehicular ad hoc networks.

1 Introduction

The emerging vehicular ad hoc network (VANET) consists of a set of vehicles and a set of stationary units along the roads, known as road-side units (RSUs), all equipped with wireless communication devices. By employing vehicle-to-vehicle and vehicle-to-RSU communications, VANETs can realize various new applications to optimize the vehicle traffic, provide infotainment to passengers, and enhance the public safety for drivers and pedestrians. Most of the VANET high priority safety applications require that each vehicle broadcasts information related to its current speed, acceleration, heading, etc., to all the vehicles within its one-hop neighbourhood [4]. Hence, supporting a reliable one-hop broadcast service is a main requirement of a medium access control (MAC) protocol for VANETs. The VeMAC protocol is based on time division multiple access (TDMA) and is recently proposed to satisfy the quality-of-service (QoS) requirements of VANET safety applications [1], [2], [5]–[7]. The protocol is developed specifically to provide a reliable one-hop broadcast service in a VANET scenario, while supporting multichannel operation to comply with the seven dedicated short range communication (DSRC) channels allocated by the Federal Communication Commission (FCC) for vehicular communications. Demonstrated by ns-2 simulations employing mobility traces of vehicles in a realistic city scenario, it is shown that the VeMAC protocol significantly outperforms the IEEE 802.11p standard [8] in satisfying the QoS requirements of periodic and event-driven safety applications in VANETs [2].

- *H. A. Omar and W. Zhuang are with the Center for Wireless Communications, Department of Electrical and Computer Engineering, University of Waterloo, 200 University Avenue West, Waterloo, Ontario, Canada, N2L 3G1. E-mail: {h3omar, wzhuang}@uwaterloo.ca*
- *L. Li is with the Communications Research Center, Ottawa, Ontario, Canada, K2H 8S2. E-mail: li.li@crc.ca*

This work is presented in part in IEEE INFOCOM 2014 [3].
This work was supported by a research grant from the Natural Science and Engineering Research Council (NSERC) of Canada.

Although safety applications are the key motivation for VANETs, the applications targeting passenger infotainment have been gaining significant interests [9]. Infotainment improves the driving experience, makes the trips more enjoyable, and may accelerate the deployment of VANETs due to a small market penetration requirement as compared to that needed for most of the safety applications [10]. One of the main infotainment services of VANETs is in-vehicle Internet access, which allows a vehicle to connect to the Internet by communicating with Internet gateways deployed along the road sides [9]. A vehicle can communicate with a gateway either directly (when they are within the communication range of each other) or via multihop communications, i.e., by using other vehicles to relay packets to/from the gateway. The first objective of this paper is to develop a new deployment technique to determine the locations of the Internet gateways on the roads, and define the maximum number of hops that a gateway can use to communicate with a certain vehicle. The proposed technique minimizes the total cost of gateway deployment, and guarantees that a vehicle can connect to an Internet gateway with a probability greater than a specified threshold. The probability that a vehicle can connect to a certain gateway is the probability of the existence of a network path between them, where the network path consists of a maximum number of hops that is determined by the proposed technique for each deployed gateway. To the best of our knowledge, no previous strategy for gateway placement has considered the existence of network paths among the vehicles and the deployed gateways. Since the existence of a network path mainly depends on the vehicle traffic conditions in the region where the gateways are deployed, we employ the cutting-edge microscopic traffic simulator VISSIM [11] to simulate the vehicle movement in the deployment region. The proposed strategy is evaluated by considering the gateway placement on the roads around the University of Waterloo (UW) campus.

In addition to the deployment strategy of Internet gate-

ways, this paper introduces a novel packet routing scheme which allows a vehicle to discover the existence of an Internet gateway and to send/receive packets to/from the gateway via multihop communications. The proposed routing scheme is designed over the VeMAC protocol to exploit some useful VeMAC features, such as the knowledge of all the nodes (vehicles and gateways) which exist in a two-hop neighbourhood. This VANET architecture aims at achieving multihop in-vehicle Internet access by using the routing scheme, while satisfying the QoS requirements of the safety applications via the VeMAC protocol. The proposed cross-layer design between the MAC and network layers is evaluated in a highway scenario by studying the end-to-end delay required to deliver a packet from a vehicle to a gateway through multiple relay vehicles. The packet queueing at each relay vehicle is considered in the end-to-end packet delay analysis. Another performance metric under consideration is the percentage of time slots per frame occupied by all the vehicles members of the same two-hop set (THS)[1], required to limit the average packet delay to below a certain threshold at each vehicle. Numerical results are presented to study the effect of different parameters, including the vehicle density and the packet arrival rate, on the performance metrics.

2 System Model and VeMAC Protocol

The VANET under consideration consists of a set of vehicles and a set of gateways placed along the road sides to provide Internet connectivity to the vehicles. The vehicles employ multihop communications to connect to the gateways, and a gateway can communicate only with the vehicles located within a maximum number of hops from the gateway. The location of each gateway and the maximum number of hops that it can use to communicate with a vehicle are determined as described in Section 3. The VANET has one control channel (CCH) for transmission of high priority safety messages and control information, and multiple service channels (SCHs) for transmission of safety and non-safety related application messages. The VeMAC protocol [2] is used by all nodes to access the communication channels, as briefly explained in the following.

Each node has two transceivers: Transceiver1 is always tuned to the CCH, while Transceiver2 switches among the SCHs. On the CCH, the time is partitioned to frames consisting of a constant number L of time slots of equal duration t, and each second contains an integer (fixed) number of frames. Each time slot is identified by the index (from 0 to $L-1$) of the time slot within a frame, and each node is identified by a unique MAC address and a set of short VeMAC identifiers (IDs), where each VeMAC ID corresponds to a certain time slot that the node is accessing per frame on the CCH. Each VeMAC ID is chosen by a node at random, included in the header of each packet transmitted in the corresponding time slot, and changed if the node detects that its ID is already in use by another node. For a certain node, x, set $\mathcal{T}_x$ denotes the set of time slots acquired by node x on the CCH, and set $\mathcal{N}_x$ is defined as the set of one-hop neighbours of node x, from which node x has received packets on the CCH in the previous L slots. Each node must acquire at least one time slot per frame on the CCH to broadcast its safety messages, organize the communications with the one-hop neighbours over the SCHs, and announce the control information necessary to manage a distributed time slot assignment on the CCH. For the purpose of time slot assignment on the CCH, each node x should broadcast the VeMAC ID(s) and the corresponding time slot(s) of each node in set $\mathcal{N}_x$, once in each frame over one of its acquired time slot(s) in set $\mathcal{T}_x$. The short length of a VeMAC ID (9 bits [2]) serves to decrease the protocol overhead as compared to broadcasting the corresponding MAC address. Now, suppose node x is just powered on and needs to acquire a time slot. By listening to the CCH for L successive time slots, node x can determine set $\mathcal{N}_x$ and the time slot(s) used by each node in $\mathcal{N}_x$. Also, since each one-hop neighbour $y \in \mathcal{N}_x$ announces the time slot(s) used by each node in $\mathcal{N}_y$, node x can determine all the time slots used by each of its two-hop neighbours, and consequently acquires one of the available time slots as described in [2]. Then, set $\mathcal{N}_x$ is updated by node x at the end of each time slot, always based on the packets received on the CCH in the previous L slots.

At each node, the packets which require transmission over the SCHs are queued and served on a first-come-first-served basis as follows. Suppose that node x needs to transmit a packet to its one-hop neighbour y on a SCH. At its first opportunity to access the CCH, node x uses the corresponding time slot in set $\mathcal{T}_x$ to announce for node y the index of the SCH over which the packet will be transmitted. Following this announcement, both of nodes x and y turn Transceiver2 to the correct SCH and exchange packets. In each time slot in $\mathcal{T}_x$, node x can announce on the CCH for a maximum of b packets to be transmitted on the same SCH (not necessarily to the same one-hop neighbour). At the start of a time slot in $\mathcal{T}_x$, if the number of queued packets is less than the constant b, referred to as the bath-size, node x does NOT wait until the number of queued packets reaches b, but announces on the CCH to transmit the existing packets on the chosen SCH. Only one SCH index can be announced by node x in a time slot on the CCH, and the batch-size b represents the maximum number of packets which can be transmitted by node x on the SCH after each announcement.

3 Gateway Placement

In order to deploy Internet gateways in a certain geographical region, the map of the region is partitioned into equal-size square areas, called cells, by overlaying a uniform square grid over the map. Each cell which cannot be traversed by a vehicle (e.g., a cell with no overlap with any part of the roads) is removed from the set of cells, and the rest of the cells are indexed from 1 to N_{cells}, where N_{cells} denotes the total number of remaining cells. Potential locations for deploying an Internet gateway are defined on the map (e.g., equally spaced along each road) and the total number of potential gateway locations is denoted by N_{gate}. The potential locations are indexed from 1 to N_{gate}, and the cost of deploying a gateway at the j^{th} location is denoted by γ_j. If a gateway is deployed at the j^{th} location, $j = 1, ..., N_{gate}$, let ρ_j denote the maximum number of hops that the gateway can use to connect to a certain vehicle, and ρ_{max} the maximum allowed value of ρ_j for any j. Given the potential gateway locations,

1. A THS is a set of nodes in which each node can reach any other node in at most two hops.

it is required to find an optimal set $\mathcal{J}$ of location indices, and determine the values of $\rho_j \ \forall j \in \mathcal{J}$. Set $\mathcal{J}$ and the corresponding ρ_j values should minimize the total cost of gateway deployment, while ensuring that the number of gateways, which a vehicle located at the i^{th} cell can connect to, is not less than a specified value denoted by ν_i, each with a probability not less than a specified threshold, denoted by $\alpha_i \in (0, 1]$, $i = 1, ..., N_{cells}$. Based on the vehicle traffic conditions in the region where the gateways are deployed, let σ_{ijk} denote the probability that a vehicle at the i^{th} cell can reach a gateway at the j^{th} position within k hops, where $i = 1, ..., N_{cells}$, $j = 1, ..., N_{gate}$, and $k = 1, ..., \rho_{max}$. The values of $\sigma_{ijk}\ \forall i, j, k$ can be calculated by using a simulation model of the vehicle traffic in the region where the gateways are deployed, as described in Subsection 6.1. For each cell i, define set β_i as the index set of all gateways which can be reached by a vehicle located in cell i within ρ_{max} hops, i.e., $\beta_i = \{j : \sigma_{ij\rho_{max}} \neq 0\}$.

The gateway deployment is formulated by binary integer programming problem (1), which has three sets of decision variables: x_j, y_{jk}, and z_{im}, where $i = 1, ..., N_{cells}$, $j = 1, ..., N_{gate}$, $k = 1, ..., \rho_{max}$, and $m \in \beta_i$ for each i. Let $x_j = 1$ iff a gateway is deployed at the j^{th} potential gateway location, and $y_{jk} = 1$ iff a gateway is deployed at the j^{th} location and has $\rho_j = k$. Therefore, objective function (1a) represents the total cost of gateway deployment. For the third set of decision variables, constraints (1b)-(1d) ensure that, a variable $z_{ij} = 1$ if [only if] a gateway is deployed at the j^{th} location and can reach a vehicle at the i^{th} cell within ρ_j hops with a probability greater than [greater than or equal to] α_i. Given this proposition, constraint (1e) guarantees that a vehicle at any cell i can communicate with at least ν_i gateways, each with a probability not less than α_i. To show the validity of the proposition, first suppose that $x_{j'} = 1$ for a certain $j' \in \{1, ..., N_{gate}\}$. Hence, constraint (1b) ensures that there exists exactly one value $k' \in \{1, .., \rho_{max}\}$ such that $y_{j'k'} = 1$, which means $\rho_{j'} = k'$. Consequently, for each cell i such that $j' \in \beta_i$, due to constraints (1c) and (1d), $z_{ij'} = 1$ if $\sigma_{ij'k'} > \alpha_i$, and $z_{ij'} = 0$ if $\sigma_{ij'k'} < \alpha_i$ (note that $\sum_{k=1}^{\rho_{max}} \sigma_{ij'k} y_{j'k} = \sigma_{ij'k'}$). If it happens that $\sigma_{ij'k'} = \alpha_i$, the value of $z_{ij'}$ can be 0 or 1 (more likely the solver let $z_{ij'} = 1$ to satisfy constraint (1e)). On the other hand, if $x_{j'} = 0$, then constraint (1b) sets $y_{j'k} = 0\ \forall k$, while constraints (1c) and (1d) set $z_{ij'} = 0\ \forall i$ such that $j' \in \beta_i$.

$$\underset{\substack{x_j, y_{jk}, z_{im} \in \{0,1\} \\ \forall i,j,k,m}}{\text{minimize}} \sum_{j=1}^{N_{gate}} \gamma_j x_j \tag{1a}$$

$$\text{subject to} \sum_{k=1}^{\rho_{max}} y_{jk} = x_j, \quad j = 1, ..., N_{gate}, \tag{1b}$$

$$z_{im} \geq \Big(\sum_{k=1}^{\rho_{max}} \sigma_{imk} y_{mk} \Big) - \alpha_i, \quad i = 1, ..., N_{cells}, m \in \beta_i, \tag{1c}$$

$$z_{im} \leq 1 + \Big(\sum_{k=1}^{\rho_{max}} \sigma_{imk} y_{mk} \Big) - \alpha_i, \quad i = 1, ..., N_{cells}, m \in \beta_i, \tag{1d}$$

$$\sum_{m \in \beta_i} z_{im} \geq \nu_i, \quad i = 1, ..., N_{cells}. \tag{1e}$$

Note that, the solution of problem (1) depends on the values of σ_{imk} in constraints (1c) and (1d), which mainly depend on the vehicle traffic conditions in the region where the gateways are deployed, as will be shown in Subsection 6.1. The traffic conditions in different situations (e.g., weekday, weekend, morning, rush hour, etc.) can be simulated by the traffic simulator which generates the σ_{imk} values, by adjusting suitable parameters such as the rate of vehicle arrivals to the road network, the probabilities of a left or right turn at intersections, the schedule of public transit buses, etc. Additionally, special incidences can be introduced in the simulation, such as an accident or a road closure, to simulate the vehicle traffic during such events. Hence, problem (1) can be solved by using the σ_{imk} values obtained from the simulator based on target vehicle traffic.

4 Routing Scheme

The proposed routing scheme consists of two main components: 1) *gateway discovery*, which determines how the vehicles discover the existence of a gateway and how they obtain the information necessary to connect to that gateway; and 2) *packet forwarding*, which defines how a packet is delivered via multihop communications from a vehicle to a gateway and vice versa.

4.1 Gateway Discovery

In order to announce for its service, a gateway, g, periodically broadcasts a gateway discovery packet (GDP) containing the necessary information that a vehicle needs to access the gateway's service, such as the network layer address of gateway g and the maximum number of hops, ρ_g, that it can use to communicate with a certain vehicle, where ρ_g is determined as described in Section 3. Before broadcasting a GDP, as mentioned in Section 2, gateway g first announces on the CCH the index of the SCH over which the GDP will be broadcasted. Accordingly, each one-hop neighbour which receives the announcement turns its Transceiver2 to the correct SCH in order to receive the GDP. Among these one-hop neighbours, a subset is chosen to re-broadcast the GDP, and so on, until the GDP initiated by gateway g propagates ρ_g hops away from the gateway. The propagation of the GDP in the network is controlled via a time-to-live (TTL) field in the GDP header, which is originally set to $\rho_g - 1$ by gateway g and decremented by each vehicle which relays the GDP. Every GDP is identified by a broadcast ID, together with the network layer address of the gateway which initiated the GDP. These two fields are used by a vehicle to discard any duplicate of a previously received GDP. At each hop, the subset of the vehicles which relay the GDP is determined as follows. Suppose that a node, x, announces for a GDP on one of its time slots, t_x, on the CCH. For each node y which receives the announcement, let $\mathcal{D}_y$ denote the set of one-hop neighbours of node y which did not receive the announcement for the GDP sent by node x. Node y does NOT relay the GDP if any of the following conditions holds:

- TTL $= 0$;
- $\mathcal{D}_y = \phi$;
- $\exists\, z \in \mathcal{N}_y \backslash \mathcal{D}_y$ such that $\mathcal{D}_y \subseteq \mathcal{N}_z$ and $|\mathcal{N}_y| < |\mathcal{N}_z|$, where $|\cdot|$ denotes the cardinality of a set;

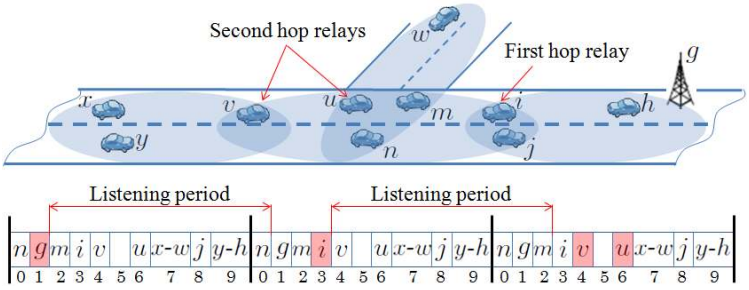

Fig. 1: The GDP relaying process based on a time slot assignment on the CCH.

- $\exists z \in \mathcal{N}_y \backslash \mathcal{D}_y$ such that $\mathcal{D}_y \subseteq \mathcal{N}_z$, $|\mathcal{N}_y| = |\mathcal{N}_z|$, and $\min_{t_z \in \mathcal{T}_z} t_z - t_x + L \times I_{(t_z < t_x)} < \min_{t_y \in \mathcal{T}_y} t_y - t_x + L \times I_{(t_y < t_x)}$, where the notation $I_{(a<b)}$ equals 1 if $a < b$ and equals 0 otherwise.

When node y receives an announcement for the GDP from node x on time slot t_x, it listens to the CCH for the $L-1$ time slots following t_x. At the end of this listening period, node y can determine sets $\mathcal{T}_z$ and $\mathcal{N}_z$ for each one-hop neighbour z (recall that, each one-hop neighbour z broadcasts the VeMAC IDs of the nodes in its $\mathcal{N}_z$ set at least once in each frame). Consequently, node y sets $\mathcal{D}_y = \{z \in \mathcal{N}_y : \text{ID}_{t_x} \text{ is not broadcasted by node } z\}$, where ID_{t_x} is the VeMAC ID of node x corresponding to time slot t_x. Consequently, node y relays the GDP if none of the mentioned conditions is true. The last condition means that, node y does not relay the GDP if it has a one-hop neighbour z which satisfies that $\mathcal{D}_y \subseteq \mathcal{N}_z$ and $|\mathcal{N}_y| = |\mathcal{N}_z|$, and which can access the CCH before node y at the end of the listening period following time slot t_x. This condition allows for a faster propagation of the GDP in the network by choosing the relay which can announce for the GDP on the CCH first.

Fig. 1 explains how a GDP broadcasted by gateway g is delivered to all the vehicles located within $\rho_g = 3$ hops from the gateway by using a few number of transmissions. In Fig. 1, a group of nodes is surrounded by an ellipse iff any two nodes in the group can reach each other in one hop (the same applies to Fig. 2). That is, the set of one-hop neighbours of a node, x, consists of all the nodes that are surrounded with node x by a certain ellipse. Fig. 1 also shows the time slot assignment on the CCH for all the nodes. Note that, different nodes may access the same time slot if they do not belong to the same THS, e.g., nodes x and w accessing time slot number 7. Each time slot that is highlighted in Fig. 1 is a time slot over which an announcement for the GDP is broadcasted. When gateway g announces for the GDP in the first frame, vehicles h, i, and j receive the announcement and listen to the CCH for a duration of 9 time slots ($L = 10$) in order to decide whether or not to relay the GDP. Vehicle h does not relay the GDP because $\mathcal{D}_h = \phi$. Similarly, vehicle j does not relay the GDP since $\mathcal{D}_j = \{m, n, u, v\} \subseteq \mathcal{N}_i$, $|\mathcal{N}_j| = |\mathcal{N}_i|$, and vehicle i can access the CCH before vehicle j at the end of the listening period. Consequently, vehicle i is the only vehicle which relays the GDP at the first hop. At the second hop, vehicles u, v, m, and n receive the GDP relayed by vehicle i. Vehicle v relays the GDP since none of its one-hop neighbours, u, m, and n (which received the GDP from vehicle i) can reach vehicles x and y in the third hop, i.e., $\nexists z \in \mathcal{N}_v \backslash \mathcal{D}_v$ such that $\mathcal{D}_v \subseteq \mathcal{N}_z$. On the other hand, among the three vehicles u, m, and n, only vehicle u relays the GDP, while vehicles m and n do not, for the same reason explained before for vehicle j. At this point, TTL $= 0$ as it has been decremented by the first and second hop relays. Hence, at the third hop, when vehicles, x, y, and w receive the GDP, none of these vehicles will relay it further. Note that, when a certain relay broadcasts the GDP, every vehicle which has previously received the same GDP can discard the relayed copy by checking the broadcast ID and the address of the initiating gateway, e.g., nodes j and h discard the GDP relayed by node i.

4.2 Packet Forwarding

The packet routing from a vehicle to a gateway is done in a proactive way. That is, each vehicle, v, stores a routing table which has an entry corresponding to each gateway g located within ρ_g hops from vehicle v. Each routing table entry at vehicle v consists of the network address of a certain gateway, the number of hops that the gateway can be reached in, and the MAC addresses of the one-hop neighbours of vehicle v which can relay a packet to the gateway. The routing table entry corresponding to a gateway, g, is created/updated during the propagation of each GDP broadcasted by gateway g, as explained in the following. Each vehicle, v, which relays a GDP initiated by gateway g includes in the relayed GDP the VeMAC IDs of a subset of its one-hop neighbours as potential vehicles which can relay a packet to gateway g. This set of potential relays included by vehicle v is denoted by $\mathcal{R}_v$, and the cardinality $|\mathcal{R}_v|$ should be limited to a certain number, denoted by $n_{\mathcal{R}}$. The set $\mathcal{R}_v$ consists of the one-hop neighbours of vehicle v which received the GDP and which can reach (in one hop) the highest number of one-hop neighbours of vehicle v which have not yet received the GDP, i.e., $\mathcal{R}_v = \{z \in \mathcal{N}_v \backslash \mathcal{D}_v : |\mathcal{R}_v| \leq n_{\mathcal{R}}, \mathcal{D}_v \cap \mathcal{N}_z \neq \phi, |\mathcal{D}_v \cap \mathcal{N}_z| \geq |\mathcal{D}_v \cap \mathcal{N}_{z'}| \, \forall z' \notin \mathcal{R}_v\}$. If vehicle v has more than one one-hop neighbour $z \in \mathcal{N}_v \backslash \mathcal{D}_v$ that have the same $|\mathcal{D}_v \cap \mathcal{N}_z| > 0$, vehicle v gives priority of inclusion in set $\mathcal{R}_v$ to the one-hop neighbours that are farther from the node from which vehicle v has received the GDP (each vehicle is aware of the positions of all its one-hop neighbours [1]). The reason is that, those one-hop neighbours are likely to be closer to the vehicles to which vehicle v is going to relay the GDP. When a vehicle, w, receives the GDP relayed by vehicle v, by calculating $\mathcal{R}_v \cap \mathcal{N}_w$, vehicle w determines the set of its one-hop neighbours which can relay a packet to gateway g. Also, by subtracting the TTL field from ρ_g, vehicle w determines the number of hops currently separating it from gateway g. Consequently, vehicle w creates/updates the entry in its routing table corresponding to gateway g. If vehicle w does not receive a GDP from gateway g for a time duration larger than a specified threshold, the entry corresponding to gateway g is removed from the routing table. The GDPs should be broadcasted by each gateway at a broadcast rate which ensures that the routing table at each vehicle is always up-to-date based on the current network topology.

Fig. 2 explains how different vehicles update their routing table entries corresponding to gateway g. When the gateway broadcasts a GDP, among all the vehicles which receive the GDP at the first hop (in the blue ellipse), only one vehicle will relay the GDP based on the relaying scheme described in Subsection 4.1. If the time slot assignment on the CCH

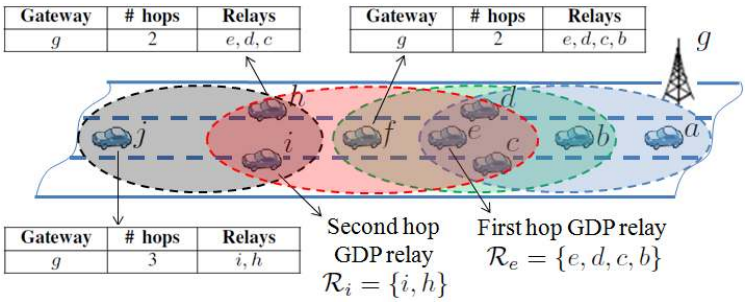

Fig. 2: Routing tables update during a GDP propagation.

requires that vehicle e is the one to relay the GDP, and if we assume that $n_{\mathcal{R}} = 4$, then vehicle e includes in the relayed GDP set $\mathcal{R}_e = \{e, d, c, b\}$. We have $\mathcal{R}_e = \{e, d, c, b\}$, because $\mathcal{D}_e = \{h, i, f\}$, $\mathcal{N}_e \backslash \mathcal{D}_e = \{e, d, c, b, a\}$, and $\mathcal{D}_e \cap \mathcal{N}_a = \phi$. When the GDP relayed by vehicle e is received by vehicles f, h, and i at the second hop (in the red ellipse), each of these vehicles finds the intersection of its $\mathcal{N}$ set with the $\mathcal{R}_e$ set, and updates the routing table entry corresponding to gateway g accordingly. Vehicle f indicates in its routing table that vehicles e, d, c, and b can relay a packet to gateway g, while each of vehicles i and h only indicates vehicles e, d, and c as potential relays (since vehicle b is not a one-hop neighbour of either vehicle i or h). Similarly, at the second hop, assuming that vehicle i decides to relay the GDP, it includes set $\mathcal{R}_i = \{i, h\}$ in the relayed GDP, which is used by vehicle j at the third hop to determine the set of possible relays to gateway g by calculating $\mathcal{R}_i \cap \mathcal{N}_j = \{i, h\}$.

To deliver a packet from a vehicle to a gateway, the vehicle forwards the packet to a randomly chosen relay among the ones listed in the routing table entry corresponding to the intended gateway. This process is repeated by each relay vehicle until the packet is finally delivered to the destination gateway. For instance, in Fig. 2, if vehicle j wants to send a packet to gateway g, by consulting its routing table, vehicle j will forward the packet to either vehicle i or vehicle h equally likely. Then, assuming that vehicle j chooses vehicle h to relay the packet, vehicle h in turn forwards the packet to a randomly chosen relay among vehicles e, d, and c, which delivers the packet directly to gateway g.

Unlike the packet routing from a vehicle to a gateway, which is done on a proactive hop-by-hop basis, packets are routed from a gateway to a vehicle on a reactive source-routing basis. That is, a source gateway includes in the header of each transmitted packet the MAC address of each vehicle which should relay the packet until it reaches the destination vehicle. This information about the whole network path to a certain vehicle, v, is provided to a gateway, g, through the packets that it receives from vehicle v. That is, each relay which forwards a packet from vehicle v to gateway g includes its MAC address in the header of the relayed packet. In this way, gateway g can find a network path to vehicle v by reversing the order of the relays in the header of the most recent packet received from vehicle v. Note that, the way that the routing table at each vehicle is built ensures that all the links on a network path from a vehicle to a gateway are bidirectional. If gateway g does not have information about the network path to a certain vehicle, or if the available network path has not been updated for a time duration larger than a specified threshold, the gateway broadcasts a route-request packet, which propagates in the network as the GDP does, until it reaches the destination vehicle. The vehicle then replies by a route-reply packet which accumulates a network path in its header while propagating back to the gateway.

5 Performance Analysis

This section investigates the end-to-end delay required to deliver a packet from a vehicle to a gateway through multiple relay vehicles. The total delay that a packet encounters at each vehicle consists of two main components: queueing delay and service delay. The queueing delay is the time duration from the instant that a packet arrives to the queue of a certain vehicle to the instant that the vehicle starts to announce for the transmission of the packet on the CCH. This delay includes the time duration that the packet spends in the queue until it becomes in the head-of-line (HOL) batch, i.e., among the first b packets, and the duration that the transmitting vehicle spends on waiting for one of its acquired time slots on the CCH (to announce the index of the SCH over which the HOL batch will be transmitted). On the other hand, the service delay of a tagged packet in the HOL batch consists of the duration of one time slot, which is used to transmit the announcement for the HOL batch on the CCH, and the time duration required to deliver the tagged packet in the HOL batch to its destination one-hop neighbour on the announced SCH. The analysis in this section neglects the second component of the packet service delay, which in general is relatively short compared to the packet queueing delay. When "delay" is mentioned solely, it refers to the total delay, which is the sum of the queueing delay and the duration of one time slot. To simplify the delay analysis, we assume that each vehicle, x, releases its time slot(s) in set $\mathcal{T}_x$ and acquires a new one(s) after each time it accesses the CCH. This assumption guarantees that, at each vehicle, the intervals of time between successive occasions of announcement for an HOL batch on the CCH are independent and identically distributed (i.i.d.) random variables. The assumption is appropriate in scenarios with high rates of transmission collisions, where the vehicles repeatedly release their time slots and acquire new ones. Consequently, each vehicle can be modeled as a queueing system with independent time intervals between successive occasions of service, where the packets are served in batches of a maximum batch-size b. In such a queuing system, when the packets arrive according to a Poisson process, we denote the system by $\mathrm{M/G^{(b)}/1}$. Hence, by considering only the arrival of packets generated at the application layer of a certain vehicle (assuming Poisson arrivals), the vehicle can be modeled as an $\mathrm{M/G^{(b)}/1}$ queueing system. However, each vehicle not only transmits the packets generated at its own application layer, but also relays the packets arriving from its one-hop neighbours. Therefore, in order to analyze the end-to-end packet delay, a network of $\mathrm{M/G^{(b)}/1}$ queues should be considered. The exact analysis of such a network of queues is extremely difficult, even when $b = 1$ [12]. Hence, to make the analysis tractable, we approximate the arrival of packets which should be relayed by a vehicle as a single Poisson process with rate parameter equal to the sum of the packet arrival rates coming to the relay vehicle from all its one-hop neighbours. That is, the superposition of the departure processes of a number, N_{input}, of $\mathrm{M/G^{(b)}/1}$ queues (representing N_{input} one-hop neighbours of a relay vehicle)

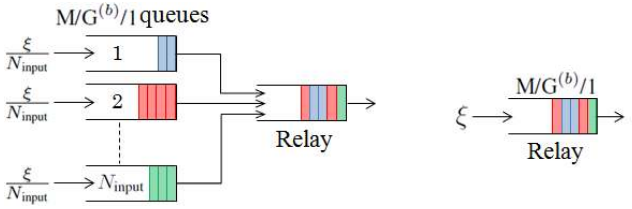

(a) Actual scenario (b) Poisson process approximation

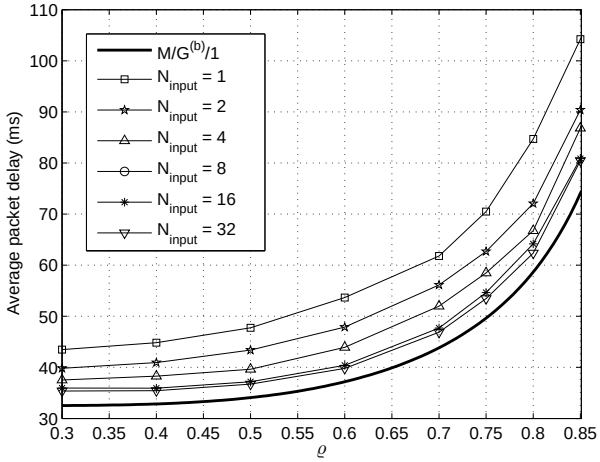

(c) Average packet delay at the relay vehicle vs. the ratio ϱ

Fig. 3: A relay vehicle with N_{input} one-hop neighbours in comparison with an M/G$^{(b)}$/1 queueing system with $b = 16$.

is approximated by a Poisson process with rate parameter $\Sigma_{i=1}^{N_{\text{input}}} \xi_i$, where ξ_i is the packet arrival rate coming from the i^{th} M/G$^{(b)}$/1 queue to the relay vehicle.

To study the accuracy of this approximation, Fig. 3 compares the average packet delay at a relay vehicle when the packets arrive to the relay according to a Poisson process with rate parameter ξ, as shown in Fig. 3b, with that in an actual case when the relay receives packets from the output of N_{input} M/G$^{(b)}$/1 queues, each with a packet arrival rate of $\frac{\xi}{N_{\text{input}}}$, as shown in Fig. 3a. For the case in Fig. 3b, the average packet delay at the relay vehicle is calculated based on the analysis of the M/G$^{(b)}$/1 queuing system (Subsection 5.3), while for that in Fig. 3a, the average delay is obtained by using MATLAB simulations, where the packets are served at the relay vehicle and at each of the N_{input} vehicles according to the VeMAC protocol. Fig. 3c shows the average packet delay at the relay vehicle versus a ratio, ϱ, which denotes the average number of packet arrivals between two successive occasions of service divided by b. As shown in Fig. 3c, for different ϱ values, the average packet delay of the M/G$^{(b)}$/1 queue represents a lower bound on the average delay when the packets arrive to the relay from N_{input} different vehicles. The lower bound becomes tighter for a large N_{input}, which indicates that the suggested Poisson process approximation is more accurate in a higher vehicle density scenario, when the packets arrive to a relay vehicle from a larger number of one-hop neighbours. Similar results are found for different values of the batch-size b. Based on the Poisson process approximation, the average packet delay at each vehicle is found by using the analysis of the M/G$^{(b)}$/1 queuing system. However, the main challenge remains in the calculation of the total packet arrival rate at a relay vehicle based on the routing scheme in Section 4, which

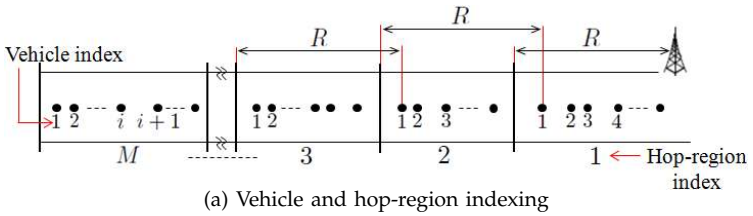

(a) Vehicle and hop-region indexing

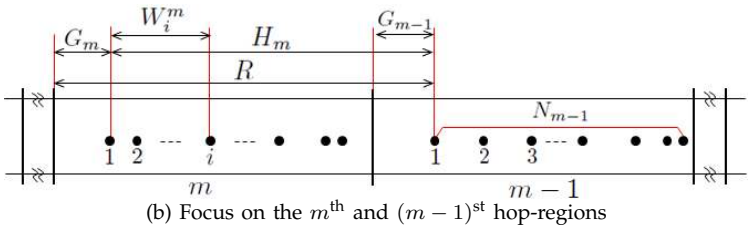

(b) Focus on the m^{th} and $(m-1)^{\text{st}}$ hop-regions

Fig. 4: Highway segment consisted of M hop-regions.

depends mainly on the network topology. In the following, a highway model is first described, then the total packet arrival rate, end-to-end-packet delay, and percentage of occupied time slots per frame are evaluated.

5.1 Highway Model

Consider a highway segment consisted of l lanes, where at any time instant the vehicles are distributed in each lane according to a Poisson process with rate parameter η_{lane} (vehicles/mile). By neglecting the width of the highway and the dimensions of a vehicle relative to the communication range, denoted by R, the vehicles are distributed along the highway according to a single Poisson process with rate parameter $\eta = l\,\eta_{\text{lane}}$, as shown in Fig. 4a (where the black dots represent vehicles). A gateway is placed at the right end of the highway segment and serves all the vehicles located within M hops of the gateway. We define M hop-regions, as shown in Fig. 4a, and assume that at any time instant there is at least one vehicle in each hop-region, i.e., there exists a network path between the gateway and each vehicle located within M hops of the gateway. The network path from any vehicle to the gateway is always up-to-date, thanks to the periodically broadcasted GDPs (Section 4.1). In each of the M hop-regions, the vehicles are indexed in an increasing order starting from the vehicle that is farthest from the gateway, as shown in Fig 4a. Based on the routing scheme in Section 4, only the first $n_{\mathcal{R}}$ vehicles in each hop-region can relay packets to/from the gateway. As illustrated in Fig. 4b, at a certain time instant, N_m denotes the number of vehicles located in the m^{th} hop-region, G_m the gap between the first vehicle in the m^{th} hop-region and the farthest edge of the region with respect to the gateway, H_m the distance separating the first vehicle in the m^{th} hop-region and that in the $(m-1)^{\text{st}}$ hop-region, and W_i^m the distance between the first vehicle in the m^{th} hop-region and the i^{th} vehicle (if exists) in the same region, where all these random variables are defined for $m = 1, ..., M$ and $i = 1, ..., \infty$ (except H_1, which is not defined). The event that N_m takes a value n_m is denoted by $\mathcal{N}_m$, and the same notation applies to all other random variables, i.e., $\mathcal{G}_m$, $\mathcal{H}_m$, and $\mathcal{W}_i^m$. Conditional on the occurrence of an event $\mathcal{E}$, the probability density function (PDF) of a continuous random variable X is denoted by $f_{X|\mathcal{E}}(x)$, the probability mass function (PMF) of a discrete random variable Y is denoted by $p(Y = y|\mathcal{E})$, and the probability of the occurrence of another event $\mathcal{E}'$ is

denoted by $p(\mathcal{E}'|\mathcal{E})$. The expected value of a random variable Z (discrete or continuous) is denoted by $\mathbb{E}(Z)$. The set of events $\mathcal{U}_{i,r}^m$, $m = 2, ..., M$, $i = 1, ..., \infty$, and $r = 1, ..., \infty$, denotes that the i^{th} vehicle in the m^{th} hop-region exists and its communication range can reach the r^{th} vehicle in the $(m-1)^{\text{st}}$ hop-region. Similarly, the set of events $\mathcal{V}_{i,r}^m$ denotes that the i^{th} vehicle in the m^{th} hop-region exists and uses the r^{th} vehicle in the $(m-1)^{\text{st}}$ hop-region as a relay to the gateway. Indicator random variable $I_{i,r}^m$ is equal to 1 whenever event $\mathcal{V}_{i,r}^m$ occurs, and is equal to 0 otherwise. Packets are generated at the application layer of each vehicle according to a Poisson process with rate parameter λ. At the r^{th} vehicle (if exists) in the m^{th} hop-region, let λ_r^m, Q_r^m, and S_r^m, $m = 1, ..., M$ and $r = 1, ..., \infty$, respectively denote the total packet arrival rate, the packet queueing delay, and the time duration (in the unit of a time slot) between successive occasions of announcement for an HOL batch on the CCH. Let D_{v}^m (D_{r}^m), $m = 1, ..., M$ ($m = 1, ..., M-1$) denote the average packet delay at a randomly chosen vehicle (relay) in the m^{th} hop-region. Also, let E^m, $m = 1, .., M$, denote the average end-to-end delay from a randomly chosen vehicle in the m^{th} hop-region to the gateway.

5.2 Total Packet Arrival Rate

The total packet arrival rate, λ_r^m, for the relay and non-relay vehicles is represented respectively by

$$\lambda_r^m = \begin{cases} \lambda + \mathbb{E}(\sum_{i=1}^{\infty} \lambda_i^{m+1} I_{i,r}^{m+1}), & 1 \le r \le n_{\mathcal{R}}, \\ & 1 \le m < M; \\ \lambda, & r > n_{\mathcal{R}} \text{ or } m = M. \end{cases} \tag{2}$$

For a relay vehicle ($1 \le r \le n_{\mathcal{R}}, 1 \le m < M$),

$$\begin{aligned} \lambda_r^m &= \lambda + \sum_{i=1}^{\infty} \lambda_i^{m+1} p(I_{i,r}^{m+1} = 1) \\ &= \lambda + \sum_{i=1}^{\infty} \lambda_i^{m+1} p(\mathcal{V}_{i,r}^{m+1}). \end{aligned} \tag{3}$$

The probability $p(\mathcal{V}_{i,r}^{m+1})$ can be found by summing the probabilities of the intersection of the event $\mathcal{V}_{i,r}^{m+1}$ with the disjoint events $\mathcal{U}_{i,k}^{m+1}$, $k = r, ..., \infty$, i.e.,

$$\begin{aligned} p(\mathcal{V}_{i,r}^{m+1}) &= p(\bigcup_{k=r}^{\infty} \mathcal{V}_{i,r}^{m+1} \cap \mathcal{U}_{i,k}^{m+1}) = \sum_{k=r}^{\infty} p(\mathcal{V}_{i,r}^{m+1} \cap \mathcal{U}_{i,k}^{m+1}) \\ &= \sum_{k=r}^{\infty} \frac{1}{\min(k, n_{\mathcal{R}})} p(\mathcal{U}_{i,k}^{m+1}), \end{aligned} \tag{4}$$

where $\min(k, n_{\mathcal{R}})$ denotes the minimum of k and $n_{\mathcal{R}}$, and $\frac{1}{\min(k,n_{\mathcal{R}})}$ represents the probability $p(\mathcal{V}_{i,r}^{m+1}|\mathcal{U}_{i,k}^{m+1})$ according to the routing scheme in Section 4, since a vehicle in the $(m+1)^{\text{st}}$ hop region is aware of a maximum of $n_{\mathcal{R}}$ relay vehicles in the m^{th} hop region and randomly chooses one among all the relay vehicles that it can reach. The probability $p(\mathcal{U}_{i,k}^{m+1})$ can be calculated for given values of the random variables N_{m+1}, G_m, H_{m+1}, and W_i^{m+1} as follows:

$$p(\mathcal{U}_{1,k}^{m+1}|\mathcal{G}_m \cap \mathcal{H}_{m+1}) = \frac{\big(\eta(R - h_{m+1})\big)^{(k-1)} e^{-\eta(R-h_{m+1})}}{(k-1)!} \tag{5a}$$

$$\begin{aligned} &p(\mathcal{U}_{i,k}^{m+1}|\mathcal{N}_{m+1} \cap \mathcal{G}_m \cap \mathcal{H}_{m+1} \cap \mathcal{W}_i^{m+1}) = \\ &\frac{\big(\eta(R - h_{m+1} + W_i^{m+1})\big)^{(k-1)} e^{-\eta(R-h_{m+1}+W_i^{m+1})}}{(k-1)!}, \ i > 1. \end{aligned} \tag{5b}$$

Equations (5a) and (5b) are the probabilities of having exactly $k-1$ vehicles in a distance $R - h_{m+1}$ and $R - h_{m+1} + W_i^{m+1}$ respectively. Note that (5b) is correct provided that $n_{m+1} \ge i$, otherwise $p(\mathcal{U}_{i,k}^{m+1}|\mathcal{N}_{m+1} \cap \mathcal{G}_m \cap \mathcal{H}_{m+1} \cap \mathcal{W}_i^{m+1}) = 0$. By using (5a), (5b), and the law of total probability, $p(\mathcal{U}_{i,k}^{m+1})$ can be calculated using (9a) and (9b). The unknown PDFs and PMFs in (9) can be found as follows. The PMF $p(N_{m+1} = n_{m+1}|\mathcal{G}_m \cap \mathcal{H}_{m+1})$ is the probability of having exactly $(n_{m+1}-1)$ vehicles in a distance $h_{m+1} - g_m$, i.e.,

$$\begin{aligned} p(N_{m+1} =& n_{m+1}|\mathcal{G}_m \cap \mathcal{H}_{m+1}) = \\ &\frac{\big(\eta(h_{m+1} - g_m)\big)^{n_{m+1}-1} e^{-\eta(h_{m+1}-g_m)}}{(n_{m+1}-1)!}. \end{aligned} \tag{6}$$

The PDF $f_{G_m}(g_m)$, $m = 1, ..., M-1$, can be found in a recursive way by using [13]:

$$f_{G_1}(g_1) = \frac{\eta e^{-\eta g_1}}{1 - e^{-\eta R}}, 0 < g_1 < R \tag{7a}$$

$$\begin{aligned} f_{G_m|\mathcal{G}_{m-1}}(g_m, g_{m-1}) &= \frac{\eta e^{-\eta g_m}}{1 - e^{-\eta(R-g_{m-1})}}, \\ 0 < &g_m < R - g_{m-1}, 1 < m \le M \end{aligned} \tag{7b}$$

$$\begin{aligned} f_{G_m}(g_m) = &\int_0^{R-g_m} f_{G_m|\mathcal{G}_{m-1}}(g_m, g_{m-1}) \\ &\cdot f_{G_{m-1}}(g_{m-1})\, dg_{m-1}, 1 < m \le M. \end{aligned} \tag{7c}$$

The PDF $f_{H_{m+1}|\mathcal{G}_m}(h_{m+1}, g_m)$, $m = 1, ..., M-1$, is calculated by using [13]

$$\begin{aligned} f_{H_{m+1}|\mathcal{G}_m}(h_{m+1}, g_m) &= \frac{\eta e^{-\eta(R-h_{m+1})}}{1 - e^{-\eta(R-g_m)}}, \\ g_m < &h_{m+1} < R. \end{aligned} \tag{8}$$

Finally, the PDF $f_{W_i^{m+1}|\mathcal{G}_m \cap \mathcal{H}_{m+1} \cap \mathcal{N}_{m+1}}(w_i^{m+1}, g_m, h_{m+1}, n_{m+1})$, $m = 1, ..., M-1$ and $i = 2, ..., \infty$, is the $(i-1)^{\text{st}}$ order statistic of the uniform distribution (conditional on the existence of $n_{m+1}-1$ vehicles in a distance interval $[0, h_{m+1} - g_m]$, the locations of these vehicles are i.i.d. uniformly distributed

$$p(\mathcal{U}_{1,k}^{m+1}) = \int_0^R \int_0^{h_{m+1}} p(\mathcal{U}_{1,k}^{m+1}|\mathcal{G}_m \cap \mathcal{H}_{m+1}) \cdot f_{G_m}(g_m) \cdot f_{H_{m+1}|\mathcal{G}_m}(h_{m+1}, g_m)\, dg_m\, dh_{m+1} \tag{9a}$$

$$\begin{aligned} p(\mathcal{U}_{i,k}^{m+1}) = &\sum_{n_{m+1}=i}^{\infty} \int_0^R \int_{W_i^{m+1}}^R \int_0^{h_{m+1}-W_i^{m+1}} p(\mathcal{U}_{i,k}^{m+1}|\mathcal{N}_{m+1} \cap \mathcal{G}_m \cap \mathcal{H}_{m+1} \cap \mathcal{W}_i^{m+1}) \cdot f_{G_m}(g_m) \cdot f_{H_{m+1}|\mathcal{G}_m}(h_{m+1}, g_m) \\ &\cdot p(N_{m+1} = n_{m+1}|\mathcal{G}_m \cap \mathcal{H}_{m+1}) \cdot f_{W_i^{m+1}|\mathcal{G}_m \cap \mathcal{H}_{m+1} \cap \mathcal{N}_{m+1}}(w_i^{m+1}, g_m, h_{m+1}, n_{m+1})\, dg_m\, dh_{m+1}\, dw_i^{m+1}, \ i > 1. \end{aligned} \tag{9b}$$

random variables), i.e.,

$$f_{W_i^{m+1}|\mathcal{G}_m\cap\mathcal{H}_{m+1}\cap\mathcal{N}_{m+1}}(w_i^{m+1},g_m,h_{m+1},n_{m+1}) = \frac{(w_i^{m+1})^{i-2}(h_{m+1}-g_m-w_i^{m+1})^{n_{m+1}-i}(n_{m+1}-1)!}{(h_{m+1}-g_m)^{n_{m+1}-1}(n_{m+1}-i)!(i-2)!}. \quad (10)$$

Using (5), (6), (8), (10), the two equations (9a) and (9b) can be simplified to (19a) and (19b). By evaluating the integrals in (19) and substituting into (4) then (3), the total packet arrival rate at each vehicle can be calculated.

5.3 End-to-end Packet Delay

At the r^{th} vehicle in the m^{th} hop-region, by using λ_r^m from Subsection 5.2, the probability generating function (PGF) of the number of packet arrivals during S_r^m is denoted by $K(z)$ and given by

$$\begin{aligned} K(z) &= \sum_{i=0}^{\infty}\Big(\sum_{j=1}^{L} p(S_r^m=j)\frac{e^{-\lambda_r^m jt}(\lambda_r^m jt)^i}{i!}\Big)z^i \\ &= \sum_{j=1}^{L} p(S_r^m=j)e^{-\lambda_r^m jt(1-z)} \end{aligned} \quad (11)$$

where PMF $p(S_r^m=j)$ is given by [2]

$$p(S_r^m=j) = \begin{cases} \frac{C_{k_r^m-1}^{L-j}}{C_{k_r^m}^{L}}, & 1\le j\le L-k_r^m+1 \\ 0, & \text{elsewhere} \end{cases} \quad (12)$$

with k_r^m being the number of time slots that the r^{th} vehicle in the m^{th} hop-region acquires per frame and $C_k^n=\frac{n!}{(n-k)!k!}$. By using (11) and (12), the PGF of the number of packets in the queue just before the start of the service time of an HOL batch is denoted by $\Pi(z)$ and given by [14]

$$\Pi(z) = \frac{\sum_{j=0}^{b-1}\pi_j(z^b-z^j)}{\frac{z^b}{K(z)}-1} \quad (13)$$

where constants π_j, $j=0,...,b-1$, should be chosen such that the b zeros of the numerator cancel the b zeros of the denominator on or inside the unit circle. Hence, by using the analysis of the M/G$^{(b)}$/1 queueing system [14], we have

$$\mathbb{E}(Q_r^m) = \frac{\Pi'(1)-\lambda_r^m t\mathbb{E}(S_r^m)}{\lambda_r^m} + \frac{t\mathbb{E}((S_r^m)^2)}{2\mathbb{E}(S_r^m)} \quad (14)$$

where $\Pi'(1)=\frac{d}{dz}\Pi(z)$ evaluated at $z=1$. Finally, the expected values of D_{v}^m, D_{r}^m, and E^m are given by the following set of equations:

$$\begin{aligned} \mathbb{E}(D_{\text{v}}^m) &= \sum_{i=1}^{\infty} p(N_m=i)\frac{1}{i}\sum_{j=1}^{i}(\mathbb{E}(Q_j^m)+t), \\ &\qquad 1\le m\le M \end{aligned} \quad (15)$$

Fig. 5: A snap shot from the VISSIM simulations with the simulated roads shown in grey.

$$\begin{aligned} \mathbb{E}(D_{\text{r}}^m) &= \sum_{i=1}^{n_{\mathcal{R}}-1} p(N_m=i)\frac{1}{i}\sum_{j=1}^{i}(\mathbb{E}(Q_j^m)+t) \\ &+p(N_m\ge n_{\mathcal{R}})\frac{1}{n_{\mathcal{R}}}\sum_{j=1}^{n_{\mathcal{R}}}(\mathbb{E}(Q_j^m)+t), 1\le m\le M \end{aligned} \quad (16)$$

$$p(N_1=i) = \frac{(\eta R)^i e^{-\eta R}}{i!(1-e^{-\eta R})},\ i\ge 1 \quad (17a)$$

$$\begin{aligned} p(N_m=i) &= \int_0^R\int_0^{h_m} p(N_m=i|\mathcal{G}_{m-1}\cap\mathcal{H}_m) \\ &\quad\cdot f_{G_{m-1}}(g_{m-1})\cdot f_{H_m|\mathcal{G}_{m-1}}(h_m,g_{m-1})\,dg_{m-1}\,dh_m \\ &= \frac{\eta^i}{(i-1)!}\int_0^R\int_0^{h_m}(h_m-g_{m-1})^{i-1}\cdot e^{-\eta(R-g_{m-1})} \\ &\quad\cdot\frac{f_{G_{m-1}}(g_{m-1})}{1-e^{-\eta(R-g_{m-1})}}\,dg_{m-1}\,dh_m, \\ &\quad 1<m\le M,\ i\ge 1 \end{aligned} \quad (17b)$$

$$\mathbb{E}(E^1) = \mathbb{E}(D_{\text{v}}^1) \quad (18a)$$

$$\mathbb{E}(E^m) = \mathbb{E}(D_{\text{v}}^m) + \sum_{i=1}^{m-1}\mathbb{E}(D_{\text{r}}^i), 1<m\le M. \quad (18b)$$

5.4 Percentage of Occupied Time Slots

Based on the batch-size b and λ_r^m at the r^{th} vehicle in the m^{th} hop-region, consider that the vehicle adjusts its number of time slots per frame, k_r^m, to guarantee that the average packet delay, $\mathbb{E}(Q_r^m)+t$, is below a threshold, denoted by $d_{\max}$. This subsection studies the number of time slots per frame required by all the vehicles of the same THS in order to limit the average packet delay at each vehicle below $d_{\max}$. This number should not exceed L to avoid any hidden terminal problem and allow each vehicle to acquire a time slot on the

$$p(\mathcal{U}_{1,k}^{m+1}) = \frac{\eta^k}{(k-1)!}\int_0^R\int_0^{h_{m+1}}(R-h_{m+1})^{(k-1)}\cdot e^{-2\eta(R-h_{m+1})}\cdot\frac{f_{G_m}(g_m)}{1-e^{-\eta(R-g_m)}}\,dg_m\,dh_{m+1} \quad (19a)$$

$$p(\mathcal{U}_{i,k}^{m+1}) = \frac{1}{(k-1)!(i-2)!}\eta^{k+i-1}\int_0^R\int_0^{h_{m+1}}\int_0^{h_{m+1}-g_m} F_k(w_i^{m+1},h_{m+1})\cdot\frac{f_{G_m}(g_m)}{1-e^{-\eta(R-g_m)}}\,dw_i^{m+1}\,dg_m\,dh_{m+1},\ i>1, \quad (19b)$$

where the function $F_k(w_i^{m+1},h_{m+1}) = (w_i^{m+1})^{i-2}\cdot e^{-2\eta(R-h_{m+1}+w_i^{m+1})}\cdot(R-h_{m+1}+w_i^{m+1})^{k-1}$.

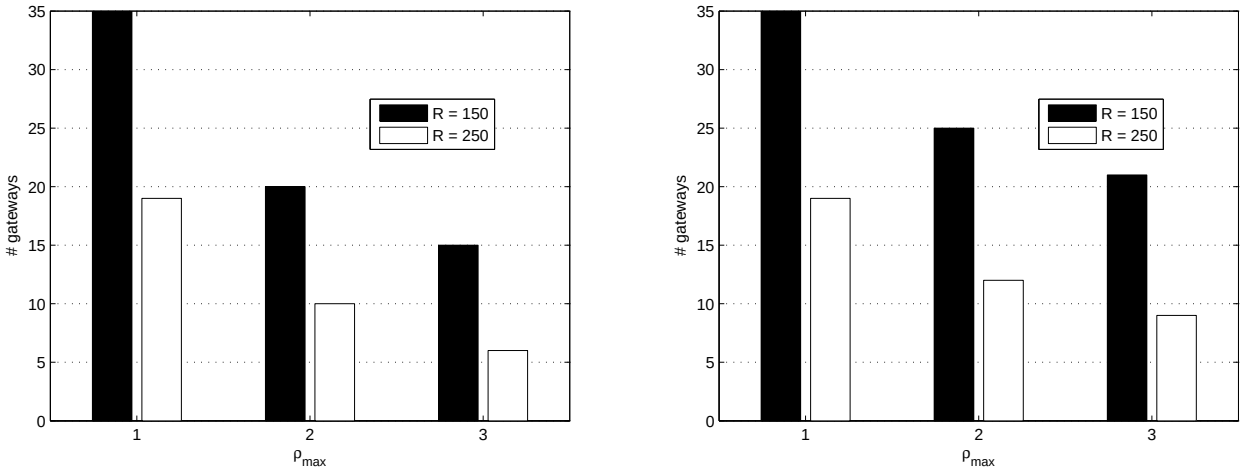

(a) High vehicle density

(b) Low vehicle density

Fig. 6: The number of deployed gateways versus ρ_{max} for $\alpha = 0.8$ and two different communication ranges.

CCH. We define $M-1$ two hop (TH) regions. The first TH region contains all the vehicles in the first and second hop-regions, while the m^{th} TH region, $m = 2, ..., M-1$, contains all the vehicles in the m^{th} and $(m+1)^{\text{st}}$ hop-regions, plus all the vehicles in the $(m-1)^{\text{st}}$ hop-region which can reach at least one vehicle in the m^{th} hop-region. Based on this definition, the number of vehicles in each of TH regions 2 to $M-1$ can be larger than the number of vehicles which actually exist in one THS. The reason is that, a vehicle in the $(m-1)^{\text{st}}$ hop-region which can reach some of the vehicles in the m^{th} hop-region is not necessarily a two-hop neighbour of all the vehicles in the $(m+1)^{\text{st}}$ hop-region. Let O_m, $m = 1, ..., M$ and T_m, $m = 1, ..., M-1$, respectively denote the total number of time slots used by all the vehicles in the m^{th} hop-region and m^{th} TH region. Also, let $\widetilde{N}_m$, $m = 1, ..., M-2$, denote the total number of vehicles in the m^{th} hop-region which can reach at least one vehicle in the $(m+1)^{\text{st}}$ hop-region, and V_m the total number of time slots used by $\widetilde{N}_m$. Hence,

$$\mathbb{E}(O_m) = \sum_{i=1}^{\infty} p(N_m = i) \sum_{j=1}^{i} k_j^m, 1 \leq m \leq M \tag{20}$$

$$\mathbb{E}(T_1) = \mathbb{E}(O_1) + \mathbb{E}(O_2) \tag{21a}$$

$$\mathbb{E}(T_m) = \mathbb{E}(O_{m+1}) + \mathbb{E}(O_m) + \mathbb{E}(V_{m-1}), 2 \leq m \leq M-1 \tag{21b}$$

$$\mathbb{E}(V_m) = \sum_{i=1}^{\infty} p(\widetilde{N}_m = i) \sum_{j=1}^{i} k_j^m, 1 \leq m \leq M-2 \tag{22a}$$

$$p(\widetilde{N}_m = i) = \sum_{j=1}^{\infty} p(N_{m+1} = j) p(\mathcal{U}_{j,i}^{m+1}) \quad 1 \leq m \leq M-2, 1 \leq i \leq \infty, \tag{22b}$$

where $p(N_m = j)$ and $p(\mathcal{U}_{j,i}^{m+1})$ are given by (17) and (19) respectively.

6 Numerical Results

6.1 Gateway Placement in a City Scenario

This subsection applies the gateway placement strategy in Section 3 for a city scenario consisting of roads around the UW campus. The map is partitioned into square cells with side length of 10 m, and the potential gateway locations are defined along each road with a separation of 10 m between two successive locations. The road network is created in the microscopic vehicle traffic simulator VISSIM, as shown in Fig 5, to simulate the movement of the vehicles in low, medium, and high vehicle density scenarios. For each scenario, the VISSIM simulator generates a trace file (listing the location of each vehicle after each simulation step) that is used by a MATLAB script to calculate the probabilities $\sigma_{i,j,k} \forall i, j, k$, as defined in Section 3. To determine whether or not a network path exists between a vehicle and gateway, the MATLAB script assumes that two nodes can communicate iff they are within the communication range of each other. Extending the script to account for the wireless channel effects, such as the shadowing caused by trees and buildings, is left as a future work. At the start of the VISSIM simulations, vehicles arrive to the road network from each possible road entry according to a Poisson process with a rate parameter that differs based on the capacity of the road and the desired vehicle density. The vehicles are left to move for a warm up period of 15 min (to avoid transient effects), then their positions are recorded for another 30 min. Each intersection is controlled by traffic lights or stop signs, depending on how the intersection is controlled in reality. At each intersection, a vehicle determines whether to turn left, right, or not to make any turn, according to a PMF that depends on the intersection, and once a vehicle reaches any end of the road network, it is removed from the simulations. The desired speed distribution is similar for all vehicle types (i.e., cars and buses), but varies from one road to another and during left and right turns. We employed the Wiedemann 74 car following model [15], which is developed for urban traffic. Default VISSIM parameters have been used for the car following and lane changing models, as well as for the maximum/desired acceleration and deceleration functions for cars and buses [16].

After calculating the probabilities $\sigma_{i,j,k}$ from the VISSIM simulations for different vehicle densities, problem (1) is solved by using the GUROBI optimizer 5.5 [17] together with the YALMIP modeling language [18]. The GUROBI optimizer combines a branch-and-bound algorithm, cutting-

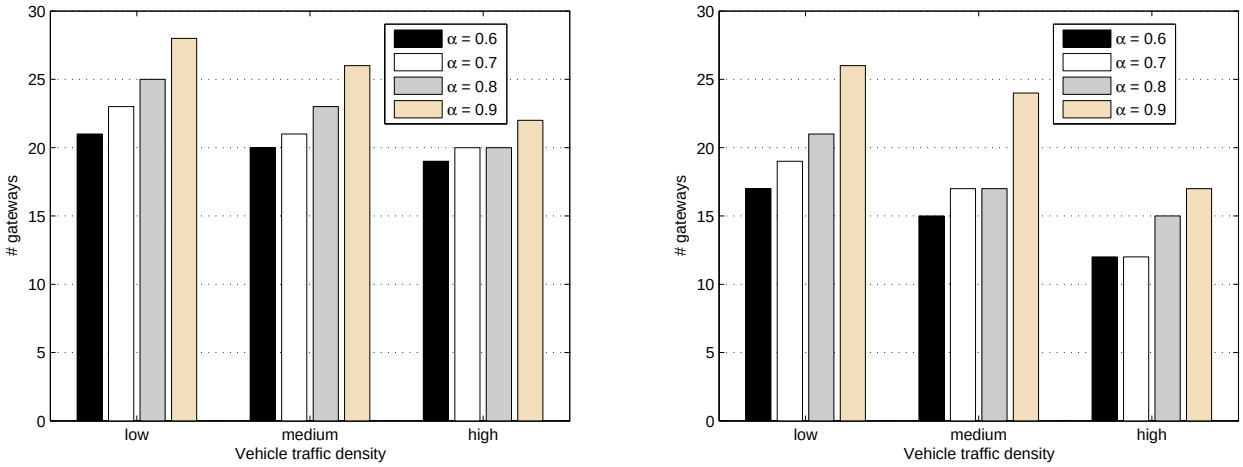

(a) $\rho_{max} = 2$ (b) $\rho_{max} = 3$

Fig. 7: The number of deployed gateways versus vehicle traffic for $R = 150$ m.

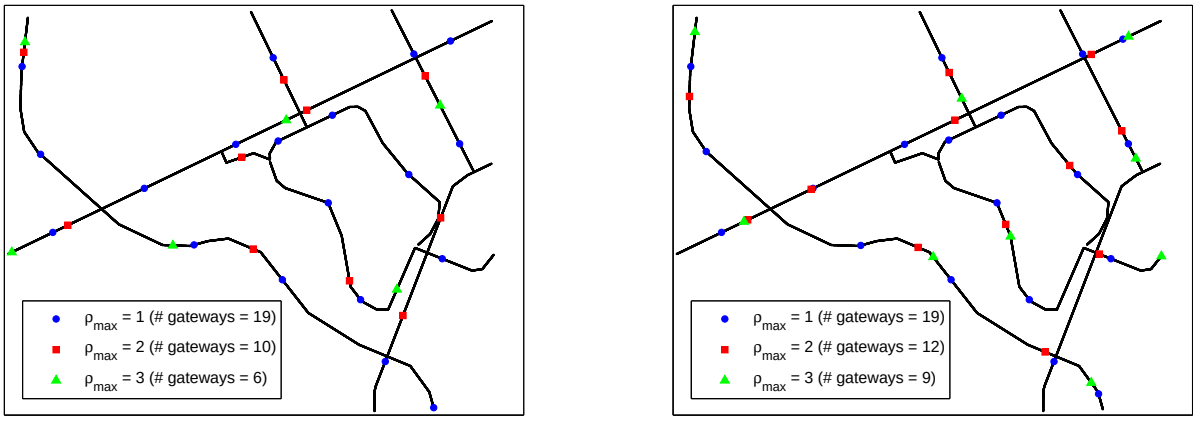

(a) High vehicle density (b) Low vehicle density

Fig. 8: The locations of the deployed gateways for $\alpha = 0.8$ and $R = 250$ m.

plane methods, and multiple heuristics in order to solve a binary integer programming problem. In problem (1), we set $\gamma_j = 1\ \forall j$ (equivalent to minimizing the number of deployed gateways), $\nu_i = 1$, and $\alpha_i = \alpha\ \forall i$, where α is a parameter ranging from 0.6 to 0.9 with step 0.1 [2]. A video showing the optimal locations of gateways in a VISSIM simulation can be found at [19].

Fig. 6 shows the effect of ρ_{max} and R on the number of deployed gateways in high and low vehicle density scenarios. As shown in Fig. 6a, when ρ_{max} is increased from 1 to 3, the number of gateways drops from 35 to 15 and from 19 to only 6 gateways for a communication range of 150 m and 250 m respectively. The effect of increasing ρ_{max} on the reduction of the number of deployed gateways is more significant in the high density scenario due to the existence of more vehicles which can relay packets to/from the gateways. For instance, as shown in Fig. 6b, when $R = 150$ m in a low density scenario, increasing ρ_{max} from 1 to 3 results in a 40% reduction of the number of deployed gateways, as compared to around 57% reduction in the high density scenario in Fig. 6a. Note that, when $\rho_{max} = 1$, the vehicle traffic density does not have any effect on the number of deployed gateways, which is the case when each cell is required to be within the communication range of at least one gateway.

The effect of the vehicle traffic density and the threshold α on the number of deployed gateways when $R = 150$ m is illustrated in Fig. 7 for $\rho_{max} = 2$ and $\rho_{max} = 3$. In each of Figs. 7a and 7b, for a given α value, the number of gateways decreases when the vehicle density increases. This decrease in the number of gateways deployed in a higher vehicle density is more remarkable when $\rho_{max} = 3$ (Fig. 7b), especially for a high α value. Similarly, for a certain vehicle density in Fig. 7a or 7b, increasing α usually requires the deployment of additional gateways. The effect of α on the number of deployed gateways is more significant in a lower vehicle density scenario and for a higher ρ_{max} value. The same results as in Fig. 7 are obtained for $R = 250$ m. When $R = 250$ m and $\alpha = 0.8$, Figs. 8a and 8b illustrate the locations of the gateways on the map for different ρ_{max} values, respectively in high and low vehicle density scenarios. It is obvious from Fig. 8 how the vehicle density affects the optimal number and locations of gateways, except when $\rho_{max} = 1$. For a gateway located at position j, the value of ρ_j assigned by the optimizer

2. The 'homogeneous' setting of the parameters $\gamma_j = 1\ \forall j$, $\nu_i = 1$, and $\alpha_i = \alpha\ \forall i$ is just to simplify the illustration of the numerical results of optimization problem (1).

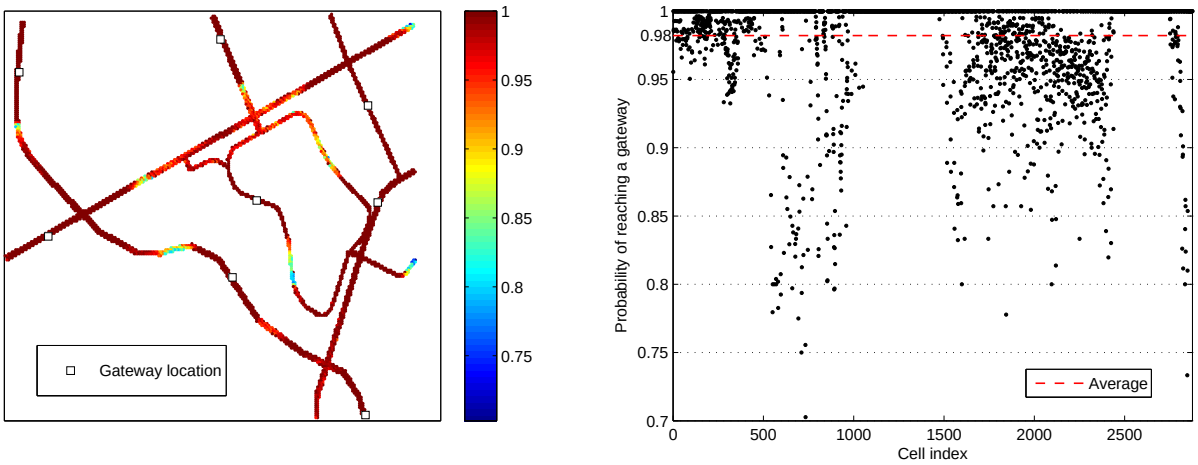

(a) Probability values indicated by the colorbar

(b) Probability values versus cell index

Fig. 9: The probability of reaching a gateway in a low traffic density for $\alpha = 0.7$, $\rho_{max} = 3$, and $R = 250$ m.

is equal to ρ_{max} almost for all j.

As the threshold α represents the minimum acceptable probability of reaching a gateway from a certain cell, the average probability (over all cells) of reaching a gateway is eventually greater than α. For instance, as shown in Fig. 9a, while $\alpha = 0.7$, for most of the cells, a vehicle can reach a gateway with a probability greater than 0.95. Hence, the average probability of reaching a gateway is around 0.98, as shown in Fig. 9b. Note that, in Fig. 9b, the cells are indexed by scanning the map from left to right (bottom-up) and, hence, close values of the indices of two cells do not necessarily mean that the cells are located in proximity of each other on the map. The cells having a probability 1 in Fig. 9b are those which are located within the communication range of a gateway. The relation between the threshold α and the average probability of reaching a gateway achieved over all cells is shown in Fig. 10 for $R = 250$ m. Even when $\alpha = 0.6$, the average probability is above 0.978 for all vehicle densities and ρ_{max} values. Similar results were found for the other communication range, $R = 150$ m.

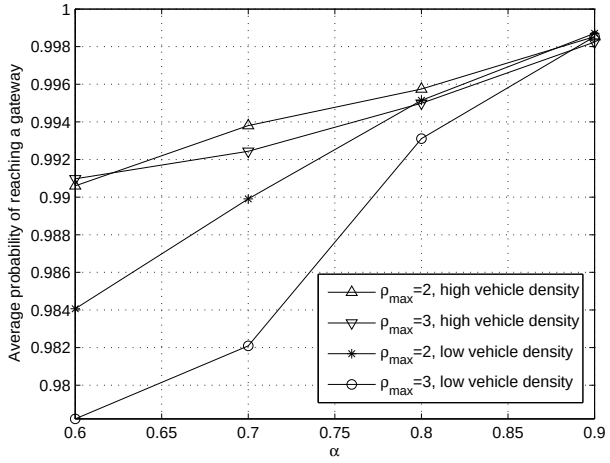

Fig. 10: The average probability of reaching a gateway versus the threshold α for $R = 250$ m.

6.2 Packet Routing in a Highway Scenario

This section presents numerical results for a 4-lane highway segment consisting of 5 hop-regions based on a communication range $R = 150$ m. The average vehicle density per lane, η_{lane}, varies from 12 to 67 vehicles/mile, a range which corresponds to traffic flow conditions varying from a free-flow scenario to a near-capacity one [20]. For the VeMAC protocol, the number of time slots per frame $L = 275$ slots and the slot duration $t = 0.35$ ms, resulting in a frame duration of 96.25 ms [2]. We use MAPLE 17 to calculate the PDFs $f_{G_m}(g_m)$, $m = 1, .., 4$, in (7), and MATLAB R2012b for all other calculations including the numerical evaluation of the integrals in (17b) and (19).

Fig. 11a shows λ_r^m, for $r = 1, ..., 10$, $m = 1, ..., 5$, and different λ values. In Fig. 11a, with $n_{\mathcal{R}} = 10$, the vehicles under consideration in hop-regions 1 to 4 represent all the potential relay vehicles located in these hop-regions. In the 5^{th} hop-region, $\lambda_r^5 = \lambda \, \forall r$, since the vehicles in this hop-region do not relay any packet. On the other hand, in the m^{th} hop region, $m = 1, ..., 4$, λ_r^m increases when the vehicle index r decreases. The reason is that, when index r is small, a relay vehicle in the m^{th} hop region is more likely to be reached by a higher number of vehicles in the $(m+1)^{\text{st}}$ hop region. Similarly, for a given vehicle index r, λ_r^m increases when the hop-region index m is smaller, i.e., when the r^{th} relay vehicle is in a hop-region closer to the gateway. The reason is that, the relay vehicles located at the m^{th} hop region ($m < 5$) will eventually relay all the packets arriving from all the farther hop-regions (indexed $m+1, ..., 5$) to the gateway. A more focused illustration of the variation of λ_r^m with r and m is shown in Fig. 11b, which concentrates only on the first three relay vehicles in each hop-region with a single λ value. The increase in the λ value eventually increases $\lambda_r^m \, \forall r, m$, as shown in Fig. 11a. Similarly, if λ remains constant and η_{lane} increases, λ_r^m increases for all the relay vehicles ($m = 1, ..., 4, r = 1, .., 10$), as illustrated in Fig. 11c.

The number $n_{\mathcal{R}}$ of relays included in the GDP defines the number of potential relay vehicles in each hop-region. Consequently, the value of $n_{\mathcal{R}}$ affects λ_r^m for some m and r, as shown in Fig. 11d. When $n_{\mathcal{R}} = 5$, only the first 5 vehicles in each hop-region can relay packets, and hence $\forall m$, the value of λ_r^m increases for $r = 1, ..., 5$ and decreases for $r = 6, ..., 15$

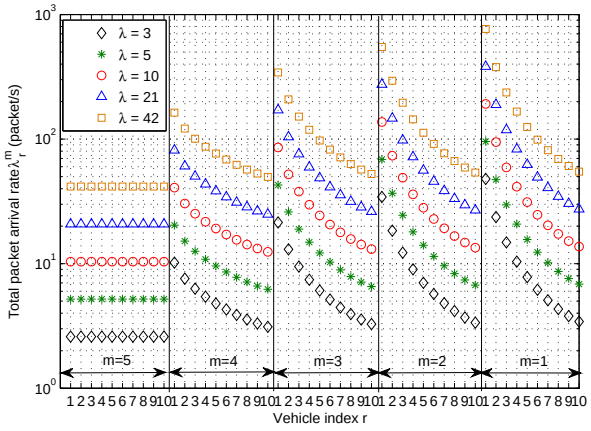

(a) First ten vehicles in each hop region for $n_{\mathcal{R}} = 10$ and $\eta_{\text{lane}} = 30$ vehicles/mile

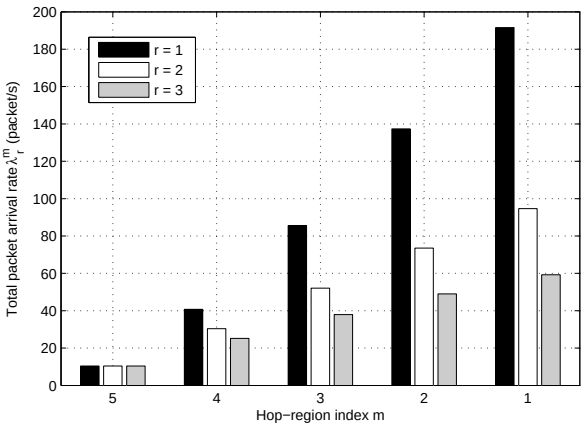

(b) First three vehicles in each hop region for $n_{\mathcal{R}} = 10$, $\eta_{\text{lane}} = 30$ vehicles/mile, and $\lambda = 10$ packet/s

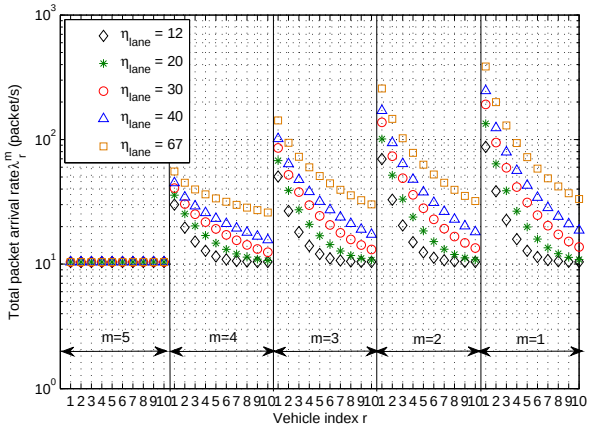

(c) First ten vehicles in each hop region for $n_{\mathcal{R}} = 10$ and $\lambda = 10$ packets/s

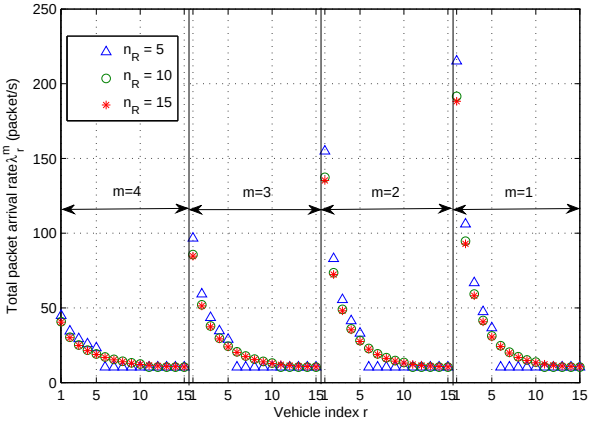

(d) First 15 vehicles in each hop region for $\eta_{\text{lane}} = 30$ vehicles/mile and $\lambda = 10$ packets/s

Fig. 11: Total packet arrival rate λ_r^m at the vehicles in each hop region.

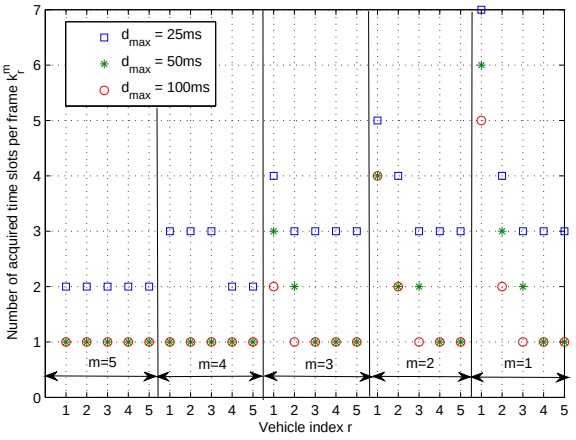

(a) $n_{\mathcal{R}} = 5$ and $b = 4$

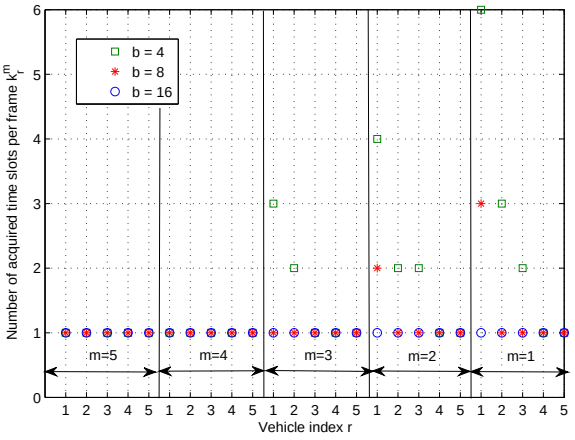

(b) $n_{\mathcal{R}} = 5$ and $d_{\max} = 50$ ms

Fig. 12: Number of acquired time slots per frame k_r^m by each of the first five vehicles in each hop-region for $\eta_{\text{lane}} = 30$ vehicles/mile and $\lambda = 10$ packets/s.

as compared to the cases of $n_{\mathcal{R}} = 10$ and $n_{\mathcal{R}} = 15$. On the other hand, no significant difference in $\lambda_r^m \, \forall r, m$ is observed when $n_{\mathcal{R}}$ is changed from 10 to 15. The reason is that, even if there are 15 potential relays included in the GDP broadcasted by a vehicle in the m^{th} hop region, not all the 15 relays can be reached by the vehicles in the $(m+1)^{\text{st}}$ hop region, and consequently not all of them will actually relay packets.

The effect of $d_{\max}$ on k_r^m is illustrated in Fig. 12a for the first five vehicles in each hop-region. When $d_{\max} = 25$ ms, while the r^{th} vehicle in the 5^{th} hop-region (does not relay packets) has $k_r^5 = 2$ slots $\forall r$, some relay vehicles in the other hop-regions need to acquire a higher number of time slots per frame in order to satisfy this delay requirement, e.g., $k_1^1 = 7$ slots. When $d_{\max}$ is increased to 100 ms, only one time

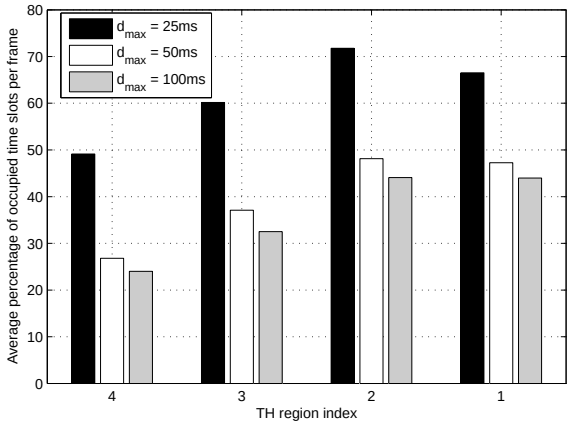

(a) $\lambda = 21$ packets/s, $n_{\mathcal{R}} = 10$, and $b = 4$

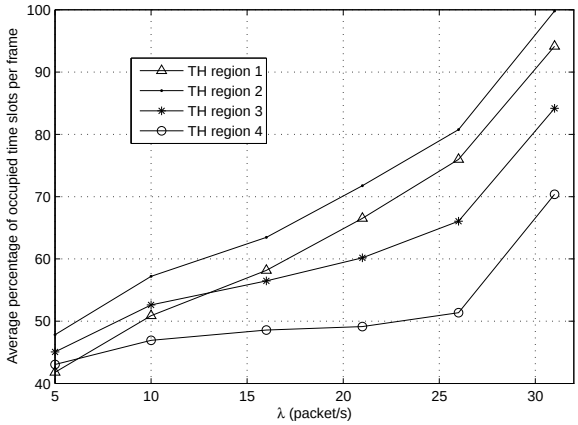

(b) $n_{\mathcal{R}} = 10$, $b = 4$, and $d_{\max} = 25$ ms

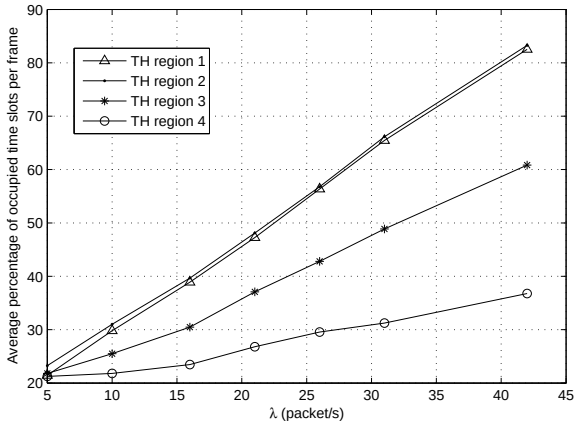

(c) $n_{\mathcal{R}} = 10$, $b = 4$, and $d_{\max} = 50$ ms

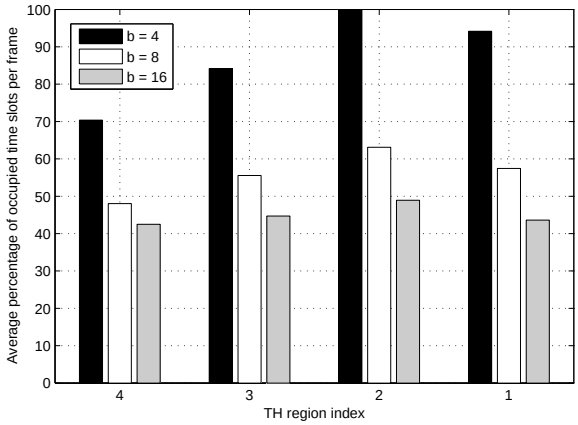

(d) $\lambda = 31$ packets/s, $n_{\mathcal{R}} = 10$, and $d_{\max} = 25$ ms

Fig. 13: Average percentage of occupied time slots per frame for each TH region for $\eta_{\text{lane}} = 67$ vehicles/mile.

slot per frame is acquired by each vehicle, except the relay vehicles with high packet arrival rates at the hop-regions close to the gateway. Fig. 12b shows that, when the batch-size b increases, the number of time slots acquired by a relay vehicle can be significantly reduced, since the vehicle is able to announce for a larger number of packets in each time slot. For instance, as shown in Fig. 12b, while a batch-size $b = 4$ requires $k_1^1 = 6$ slots and $k_1^2 = 4$ slots, both values are halved when $b = 8$, and are reduced to only 1 slot when $b = 16$.

Fig. 13a shows the effect of $d_{\max}$ on the average percentage of time slots per frame occupied by all the vehicles in each TH region, i.e., $\frac{\mathbb{E}(T_m)}{L} \times 100, m = 1, ..., 4$. Based on the TH region definition in Subsection 5.4, and given the number of time slots acquired by individual vehicles in Fig. 12, the second TH region is the most loaded (in terms of time slot occupancy) since it includes all the vehicles in the second and third hop-regions, as well as all the relay vehicles in the first hop-region. As shown in Fig. 13a, the second TH region has an average time slot occupancy less than 75%, even for $d_{\max} = 25$ ms and $\eta_{\text{lane}} = 67$ vehicles/mile. In Fig. 13a, when $d_{\max} = 25$ ms, each non-relay vehicle needs to acquire three time slots per frame, which results in a significant increase in the average slot occupancy in all TH regions, as compared with the $d_{\max} = 50$ ms and $d_{\max} = 100$ ms cases, in which a non-relay vehicle needs to acquire only two time slots per frame to satisfy the delay threshold. When $d_{\max}$ decreases from 100 ms to 50 ms, the slight increase in the average slot occupancy shown in Fig. 13a is because of the extra time slots acquired by some relay vehicles. Fig. 13b shows the average percentage slot occupancy for each TH region versus λ. When $\lambda = 31$ packets/s (3 packets/frame), almost 100% average slot occupancy is achieved at the second TH region. Hence, for the highest average vehicle density, $\eta_{\text{lane}} = 67$ vehicles/mile, smallest delay threshold, $d_{\max} = 25$ ms, and smallest batch-size, $b = 4$, under consideration, a frame length of 275 time slots can accommodate all the vehicles in each TH region for a packet arrival rate λ up to 31 packets/s. If $d_{\max}$ is increased to 50 ms, as shown in Fig. 13c, then for the same η_{lane} and b values as in Fig. 13b, the average percentage of occupied time slots remains below 85% for all TH regions, even for λ as high as 42 packets/sec (4 packets/frame). On the other hand, if $d_{\max} = 25$ ms and b is increased from 4 to 8, the average slot occupancy is reduced by approximately 35% for each TH region, as shown in Fig. 13d.

Fig. 14a shows the average end-to-end packet delay for each hop-region, $\mathbb{E}(E^m)$, $m = 1, ..., 5$, for different values of $d_{\max}$. A packet sent from a vehicle in the 5$^{\text{th}}$ hop-region can be delivered to the gateway with an average end-to-end delay of 110 ms (178 ms) when $d_{\max} = 25$ ms ($d_{\max} = 50$ ms). Note that, the value of $d_{\max}$ represents the delay threshold below which each vehicle limits its average packet delay by acquiring a suitable number of time slots per frame. How

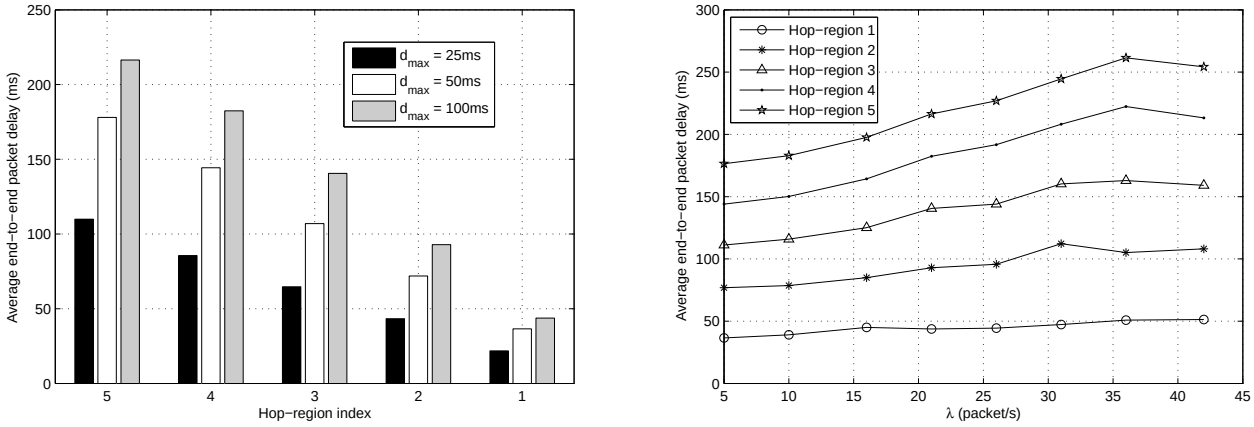

(a) $\lambda = 21$ packets/s and $b = 4$

(b) $b = 4$ and $d_{\max} = 100$ ms

Fig. 14: Average end-to-end packet delay for each hop-region for $n_{\mathcal{R}} = 10$ and $\eta_{\text{lane}} = 30$ vehicles/mile.

much the actual value of the average packet delay at a certain vehicle is below $d_{\max}$ depends mainly on the total packet arrival rate at the vehicle. Fig. 14b shows the effect of λ on the average end-to-end packet delay for each hop-region. As shown in Fig. 14b, the increase in the average end-to-end packet delay with λ is higher when a hop-region is farther from the gateway. However, the effect of λ on the average end-to-end packet delay is not significant, especially for the first two hop-regions, since when λ increases, each vehicle can access more time slots per frame in order to keep its average packet delay below $d_{\max}$. In other words, increasing λ affects more the percentage of occupied time slots per frame rather than the end-to-end packet delay as shown in Figs. 13b, 13c, and 14b.

7 Conclusions and Future Work

This paper presents a new Internet gateway placement strategy, together with a novel packet routing scheme based on the VeMAC protocol, in order to provide Internet connectivity for the vehicles by using multihop communications in a multichannel VANET. The Internet gateways are deployed in a way which minimizes the total deployment cost, subject to location-dependant lower bounds on the probability that a vehicle can find a network path to a gateway, based on the traffic conditions in the deployment region. How each vehicle discovers the existence of a gateway has been defined and how the packets are delivered between a vehicle and a gateway through multiple relay vehicles has been described. Numerical results show that, due to a high total packet arrival rate, a relay vehicle may need to acquire more time slots per frame in order to limit its average packet delay below a certain threshold, especially when the relay vehicle is located close to a gateway. By properly adjusting the number of time slots that each vehicle acquires per frame, increasing the packet arrival rate at each vehicle affects more the percentage of occupied time slots per frame rather than the end-to-end packet delay. In the future, the routing scheme proposed over the VeMAC protocol should be evaluated by using realistic mobility traces of vehicles in highway and city scenarios, in comparison with a bench mark routing protocol, such as the Greedy Perimeter Stateless Routing (GPSR), over the IEEE 802.11p standard. Also, suitable gateway selection and handover schemes should be developed, analysis of the channel utilization and end-to-end packet delivery delay should be done for larger road networks with multiple deployed gateways, and results of the gateway placement strategy should be obtained by taking into consideration the effects of the wireless channel.

Acknowledgments

We would like to thank Alexander Leung (an Undergraduate Research Assistant) for his help in calculating the probabilities σ_{imk} in problem (1), by using the vehicle trace files from VISSIM. We also would like to thank the reviewers for their comments and suggestions which helped to improve the quality of this paper.

References

[1] H. A. Omar, W. Zhuang, and L. Li, "VeMAC: A TDMA-based MAC protocol for reliable broadcast in VANETs," *IEEE Trans. Mobile Comput.*, vol. 12, no. 9, pp. 1724–1736, Sept. 2013.

[2] H. A. Omar, W. Zhuang, A. Abdrabou, and L. Li, "Performance evaluation of VeMAC supporting safety applications in vehicular networks," *IEEE Trans. Emerg. Topics Comput.*, vol. 1, no. 1, pp. 69–83, Jun. 2013.

[3] H. A. Omar, W. Zhuang, and L. Li, "On multihop communications for in-vehicle Internet access based on a TDMA MAC protocol," in *Proc. IEEE INFOCOM*, Apr. 2014.

[4] "Vehicle safety communications project task 3 final report," The CAMP Vehicle Safety Communications Consortium, Tech. Rep. DOT HS 809 859, Mar. 2005.

[5] H. A. Omar, W. Zhuang, and L. Li, "Delay analysis of VeMAC supporting periodic and event-driven safety messages in VANETs," in *Proc. IEEE GLOBECOM*, Dec. 2013.

[6] H. A. Omar, W. Zhuang, and L. Li, "Evaluation of VeMAC for V2V and V2R communications under unbalanced vehicle traffic," in *Proc. IEEE VTC2012-Fall*, Sep. 2012.

[7] H. A. Omar, W. Zhuang, and L. Li, "VeMAC: a novel multichannel MAC protocol for vehicular ad hoc networks," in *Proc. IEEE INFOCOM MobiWorld 2011*, Apr. 2011, pp. 413–418.

[8] *IEEE Std 802.11p-2010*, pp. 1–51, Jul. 15, 2010.

[9] R. Baldessari *et al.*, "Car-2-car communication consortium manifesto," Tech. Rep. Version 1.1, Aug. 2007.

[10] W. Specks *et al.*, "Car-to-car communication–market introduction and success factors," in *Proc. 5th European Congress and Exhibition on Intelligent Transport Systems and Services*, 2005.

[11] http://vision-traffic.ptvgroup.com/en-uk/products/ptv-vissim/.

[12] D. Bertsekas and R. Gallager, *Data networks*. Upper Saddle River, NJ, USA: Prentice-Hall, Inc., 1987.

[13] Y.-C. Cheng and T. Robertazzi, "Critical connectivity phenomena in multihop radio models," *IEEE Trans. Commun.*, vol. 37, no. 7, pp. 770–777, 1989.
[14] N. Bailey, "On queueing processes with bulk service," *J. R. Stat. Soc. Ser. B Stat. Methodol.*, vol. 16, no. 1, pp. 80–87, 1954.
[15] R. Wiedemann, "Modeling of RTI-Elements on multi-lane roads," in *Advanced Telematics in Road Transport, Proc. the Drive Conference*, Feb. 1991.
[16] PTV Planung Transport Verkehr AG, *VISSIM 5.40-User Manual*, 2012.
[17] http://www.gurobi.com/.
[18] J. Löfberg, "YALMIP: A toolbox for modeling and optimization in MATLAB," in *Proc. of the CACSD Conference*, Taipei, Taiwan, 2004. [Online]. Available: http://users.isy.liu.se/johanl/yalmip
[19] http://youtu.be/zaLJWfTHG8s.
[20] A. D. May, *Traffic flow fundamentals*. Englewood Cliffs, N.J: Prentice Hall, 1990.

Hassan Aboubakr Omar (S'11-M'14) received the Ph.D. (2014) degree in Electrical and Computer Engineering from the University of Waterloo, Canada, the M.Sc. (2009) degree in Engineering Mathematics and the B.Sc. degree (2005) in Electronics and Communications Engineering, both from Cairo University, Egypt. From 2005 to 2008, he was a Research Assistant at the Science and Technology Research Center, at the American University in Cairo. Since 2014, he has been working as a Postdoctoral Fellow at the University of Waterloo's Department of Electrical and Computer Engineering. Dr. Omar is the recipient of the Best Paper Award from the IEEE Globecom 2013, and his current research interest includes vehicular ad hoc networks (VANETs), heterogeneous networks (HetNets), and optimization.

Weihua Zhuang (M'93-SM'01-F'08) has been with the Department of Electrical and Computer Engineering, University of Waterloo, Canada, since 1993, where she is a Professor and a Tier I Canada Research Chair in Wireless Communication Networks. Her current research focuses on resource allocation and QoS provisioning in wireless networks, and smart grid. She is a co-recipient of the Best Paper Awards from the IEEE Globecom 2012 and 2013, the IEEE International Conference on Communications (ICC) 2007, 2012, and 2014, IEEE Multimedia Communications Technical Committee in 2011, IEEE Vehicular Technology Conference (VTC) Fall 2010, IEEE Wireless Communications and Networking Conference (WCNC) 2007 and 2010, and the International Conference on Heterogeneous Networking for Quality, Reliability, Security and Robustness (QShine) 2007 and 2008. She received the Outstanding Performance Award 4 times since 2005 from the University of Waterloo, and the Premiers Research Excellence Award in 2001 from the Ontario Government. Dr. Zhuang was the Editor-in-Chief of IEEE Transactions on Vehicular Technology (2007-2013), the Technical Program Symposia Chair of the IEEE Globecom 2011, and an IEEE Communications Society Distinguished Lecturer (2008-2011). She is a Fellow of the IEEE, a Fellow of the Canadian Academy of Engineering (CAE), a Fellow of the Engineering Institute of Canada (EIC), and an elected member in the Board of Governors of the IEEE Vehicular Technology Society (2012-2014).

Li Li (M'03-SM'14) received the M.Sc. (1990) degree in Electrical Engineering from Southeast University, Nanjing, China and Ph.D (1993) degree in Electrical Engineering from University of Ottawa, Ottawa, ON, Canada. From 1993 to 1999, she was with Nortel Networks Ltd. as a system architect and then product manager. From 1999 to 2003, she was the chief architecture at SS8 Networks Inc. Since 2003, she has been with Communications Research Centre (CRC), Ottawa, ON, Canada, where she is a research scientist. She has contributed previously to ITU-T and IETF standard working groups, co-authored IETF RFC and has been awarded with several US patents. Her current research focuses on mobile tactical radio networking and adaptive networks, with particular interests in mobile network optimization, networking protocols and algorithms, and performance modeling of mobile networks. She has served as an Associated Editor for Springer's Journal on Peer-to-peer Networking and Applications. Dr. Li has served as Co-chair for the IEEE PERCOM MP2P'06-08 workshops, track co-chair for IEEE VTC2010-Fall, session co-chair for IEEE MILCOM'08-11, and track co-chair for IEEE MILCOM 2012. She is an Associate Editor for IEEE Transactions on Vehicular Technology.